Available online at www.sciencedirect.com
SCIENCE DIRECT®
Journal of Fluorine Chemistry 125 (2004) 1657–1661
JOURNAL OF FLUORINE CHEMISTRY
www.elsevier.com/locate/fluor

Surface fluorination of the cathode active materials for lithium secondary battery

Susumu Yonezawa*, Masahiro Yamasaki, Masayuki Takashima

Department of Materials Science and Engineering, Faculty of Engineering, University of Fukui, Bunkyo 3-9-1, Fukui 910-8507, Japan

Available online 5 November 2004

Abstract

$LiMn_2O_4$ was treated with F_2 at room temperature (RT), 373 and 473 K under 1.3, 6.6 and 13.2 kPa-F_2. XPS data indicate that two kinds of fluorine species may exist on the sample surface and the ratio of these fluorines is affected by choosing the reaction condition. The peak indicating Mn^{n+} bonded to fluorine appeared in the XPS spectra of Mn2p3/2 electron. From the results of the charge/discharge measurements, the efficiency of charge/discharge process for the sample fluorinated under 1.3, 6.6 and 13.2 kPa-F_2 below 373 K was larger than that of untreated one. The discharge capacity of the fluorinated sample was also larger than that of untreated one. The discharge capacity, the loss of discharge capacity during 50 charge/discharge cycles, F/O ratio measured from XPS data and the intensity of the peak indicating Mn^{n+} bonded to fluorine in the XPS spectra were closely related to each other. The optimal fluorination condition was under 1.3 kPa-F_2 at RT for 1 h.

Keywords: Lithium secondary battery; $LiMn_2O_4$; F_2; Cyclic voltammetry; Charge/discharge test

1. Introduction

Lithium secondary battery has been widely studied because of a large terminal voltage and a large energy density. The larger capacity and the higher discharge potential are needed because the electronic mobile equipments are minimized. Lithium containing transition metal oxides, $LiCoO_2$, $LiNiO_2$, $LiMn_2O_4$ and their derivatives have been investigated to obtain the high performance cathode active materials of lithium secondary battery mainly from the view of the partial cation substitution [1–7]. In our previous study, the surface modification of these oxides with fluorine or fluorine/carbon nanocomposite by using NF_3 has been reported [8–10]. The modification of the surface of the cathode active material must have strongly effects on the battery performance because the electrochemical reaction takes place at the interface among the active material, carbon as the electroconductive material and the electrolyte. There is a paper on the modification of the surface of the active material by introducing some metals [11]. No paper, however, is found on the modification of the cathode material surface by fluorine. Unique surface properties such as higher solvation ability and polarizability (mentioned as follows) may be achieved by introducing fluorine onto the surface of the oxides because fluorine has the larger electronegativity than oxygen. In the charge/discharge process, Li^+ ion transfers between a cathode material (solid phase) and an electrolyte solution (liquid phase). The solvation/desolvation of Li^+ ion occurs at the surface of the active material because Li^+ ion exists as a solvated state in an electrolyte solution. Since the metal–fluorine (M–F) bond is more polarized than the metal–oxygen (M–O) bond, the affinity for polar electrolyte solution may be improved at the fluorinated surface of active material. Therefore, the transfer of Li^+ ion between the solid and the liquid phases may easily proceed. Furthermore, HF is produced by hydrolysis of the supporting salts such as $LiPF_6$ with a small amount of residual water contained in the electrolyte solution. HF attacks the M–O bond and water is then reproduced, so that these reactions may be repeated alternatively. In contrast, the M–F bond is unable to be attacked by HF and hence the

* Corresponding author. Tel.: +81 776 27 8910; fax: +81 776 27 8614.
E-mail address: yonezawa@matse.fukui-u.ac.jp (S. Yonezawa).

0022-1139/$ – see front matter © 2004 Elsevier B.V. All rights reserved.
doi:10.1016/j.jfluchem.2004.09.004

active materials having the fluorinated surface are expected to be stable in the electrolyte solution containing $LiPF_6$. Several papers on the fluorination of anode carbon materials reported that both the hydrophilic and hydrophobic surfaces can be generated by fluorination under the controlled conditions [12–14]. In our previous papers, it was reported that fluorine is introduced to the surface of metal oxides by the reactions with NF_3, ClF_3, etc. [15–17]. In this paper, the effect of surface fluorination of $LiMn_2O_4$ by F_2 gas on the electrochemical properties has been reported.

2. Results and discussion

Fig. 1 shows SEM photographs of $LiMn_2O_4$ untreated and treated with F_2 gas. No change was observed in the shape and morphology of the surface of $LiMn_2O_4$ particles. No change was found in the surface area and the average particle size by fluorination. The fluorination did not change the particle shape on micron scale. Fig. 2 shows XRD profiles of $LiMn_2O_4$ untreated and treated with 1.3 kPa-F_2 gas at room temperature (RT), 373 and 473 K. All peaks were indexed by using the crystal structure of spinel $LiMn_2O_4$. The Miller indices were shown in the figure. There was no extra peak in the profiles even after $LiMn_2O_4$ reacted with 1.3 kPa-F_2 gas at 473 K. But the intensity and the peak shape slightly changed after the fluorination at 473 K. The peaks around 36° in Fig. 2 were magnified in Fig. 3. There was no change in the intensity and FWHM of the peak for $LiMn_2O_4$ untreated and treated with 1.3 kPa-F_2 at RT and 373 K. The peak for $LiMn_2O_4$ treated with 1.3 kPa-F_2 at 473 K, however, has been smaller and broader than that for the other three samples. The same result was observed in case of the other peaks in Fig. 2. It was found that the fluorination of $LiMn_2O_4$ with 1.3 kPa-F_2 at the temperature lower than 373 K change only the surface state of $LiMn_2O_4$ particle. In case of $LiMn_2O_4$ fluorinated with 1.3, 6.6 and 13.2 kPa-F_2 at RT, there was no change in their XRD profiles (not shown here). The temperature is an important factor for the fluorination of $LiMn_2O_4$ surface.

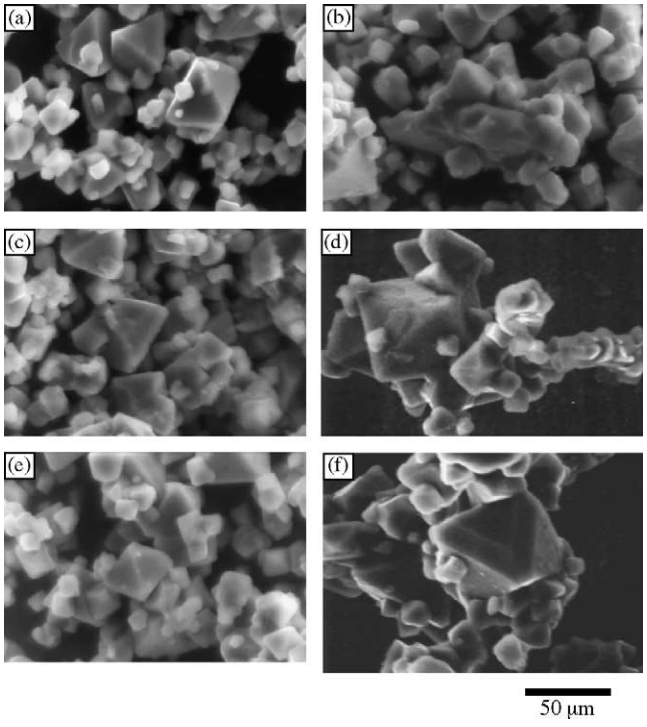

Fig. 1. SEM of $LiMn_2O_4$ untreated (a) and treated with 1.3 kPa-F_2 at 373 K (b), 1.3 kPa-F_2 at 473 K (c), 1.3 kPa-F_2 at room temperature, RT (d), 6.6 kPa-F_2 at RT (e), 13.2 kPa-F_2 at RT (f).

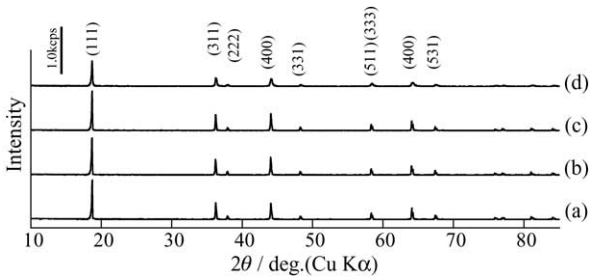

Fig. 2. XRD profiles of $LiMn_2O_4$ untreated (a) and treated with 1.3 kPa-F_2 at room temperature, RT (b), 1.3 kPa-F_2 at 373 K (c), 1.3 kPa-F_2 at 473 K (d).

XPS spectra of F1s electron for $LiMn_2O_4$ treated with 1.3 kPa-F_2 at various temperatures were shown in Fig. 4. Even at RT, the surface of $LiMn_2O_4$ reacted with 1.3 kPa-F_2 and fluorine was introduced at its surface. The peak top position of $LiMn_2O_4$ fluorinated at 473 K in Fig. 4(A) was different from that of $LiMn_2O_4$ fluorinated at RT and 373 K. Because the peak shape was asymmetric in Fig. 4, there must be at least two peaks. It was found by curve fitting that the peak in Fig. 4 was composed of two peaks at 685.4 and 687.5 eV as shown I and II in Fig. 4, respectively. The 685 eV is the binding energy for ionic F^- in the solid samples such as alkali metal fluorides. So, the peak I may correspond to F^- having interaction with correlated to Li^+ in the sample. On the other hand, it is very difficult to explain the origin of the peak at around 687.5 eV. Though F^- in

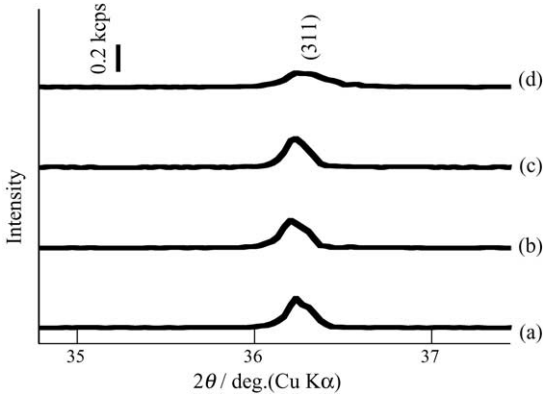

Fig. 3. XRD profiles (enlarged between 35 and 37° in Fig. 2) of $LiMn_2O_4$ untreated (a) and treated with 1.3 kPa-F_2 at room temperature, RT (b), 1.3 kPa-F_2 at 373 K (c), 1.3 kPa-F_2 at 473 K (d).

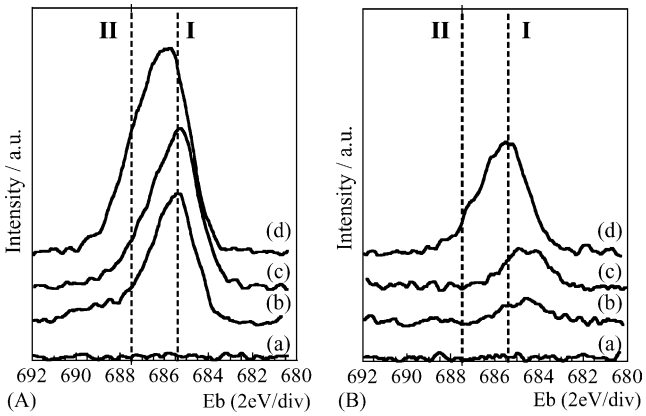

Fig. 4. XPS spectra of F1s electron in $LiMn_2O_4$ untreated (a) and treated with 1.3 kPa-F_2 at room temperature, RT (b), 1.3 kPa-F_2 at 373 K (c), 1.3 kPa-F_2 at 473 K (d) ((A) before and (B) after Ar^+ etching).

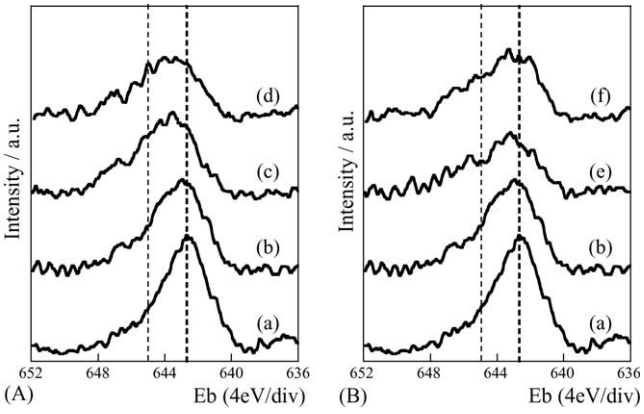

Fig. 6. XPS spectra of Mn2p3/2 electron in $LiMn_2O_4$ untreated (a) and treated with 1.3 kPa-F_2 at room temperature, RT (b), 1.3 kPa-F_2 at 373 K (c), 1.3 kPa-F_2 at 473 K (d), 6.6 kPa-F_2 at RT (e), 13.2 kPa-F_2 at RT (f) ((A) reaction temperature dependence, (B) F_2 pressure dependence).

MnF_2 has the peak at 688 eV, there is no possible reaction in which divalent manganese could be generated in case of the reaction with F_2 gas (oxidation). Since LiF has no peak at around 688 eV, the peak at 687.5 eV must correspond to the fluorine bonded to Mn^{n+} in the $LiMn_2O_4$. After argon ion etching, the peak intensity decreased as shown in Fig. 4(B). Especially the peak II diminished. In case of $LiMn_2O_4$ fluorinated at 473 K, the peak II still remained and the intensity of the peak I was very large. Considering the results of XRD measurement together, it seems that the fluorine diffuses into the inner part of the $LiMn_2O_4$ particle in this case. Fig. 5 shows XPS spectra of F1s electron in $LiMn_2O_4$ fluorinated with 1.3, 6.6 and 13.2 kPa-F_2 at RT. The intensity and the shape of the peaks were similar to each other in contrast to the result for $LiMn_2O_4$ fluorinated with 1.3 kPa-F_2 at 473 K. After argon ion etching, the peak intensity decreased similarly as shown in Fig. 5 (B). XPS spectra of Mn2p3/2 electron in $LiMn_2O_4$ fluorinated under various conditions were shown in Fig. 6. The dependence of Mn2p3/2 peaks on the temperature and F_2 pressure is shown in Fig. 6(A) and (B), respectively. In Fig. 6(a) (untreated one), only one peak was detected at 643 eV which corresponded to Mn–O bonding. From the view point of crystal structure and chemical formula, there must be at least two peaks in the profile. The signal intensity was, however, so small that it was difficult to find one more peak in Fig. 6(a). With increasing fluorination temperature, the peak at around 645 eV which corresponded to Mn–F bonding appeared in the profiles (Fig. 6(b)–(d)). Because the peak around 645 eV appeared after fluorination, Mn^{n+} which is more ionic has been produced by fluorination. Increasing the F_2 pressure, the peak around 645 eV also appeared in the profiles (Fig. 6(b), (e), (f)). More ionic Mn^{n+} was also observed in this case. The intensity ratio of the peak at 645 eV to that at 643 eV, I_{645}/I_{643} is a measure showing the progress of fluorination though the total peak intensity decreased with increasing temperature and F_2 pressure. The values of I_{645}/I_{643} were in the order of (b) < (e), (c) < (f) < (d). From these results, the fluorination of $LiMn_2O_4$ particle progressed further in the order of (b) < (e), (c) < (f) < (d). It seems that the peak I and II in Figs. 4 and 5 correspond to the fluorine mainly correlated with lithium and manganese, respectively, because only one new peak at 645 eV corresponds to Mn–F bonding appeared in XPS spectra of Mn2p3/2 electron after fluorination. The peak position in XPS spectra of O1s electron in $LiMn_2O_4$ (not shown here) tended to shift for higher binding energy. By the fluorination, O–F bonding might form or Mn–O bonding character might change. But the accurate measurement of XPS spectra of O1s electron was so difficult that the detailed discussion about the electronic state of oxygen in $LiMn_2O_4$ could not be carried out.

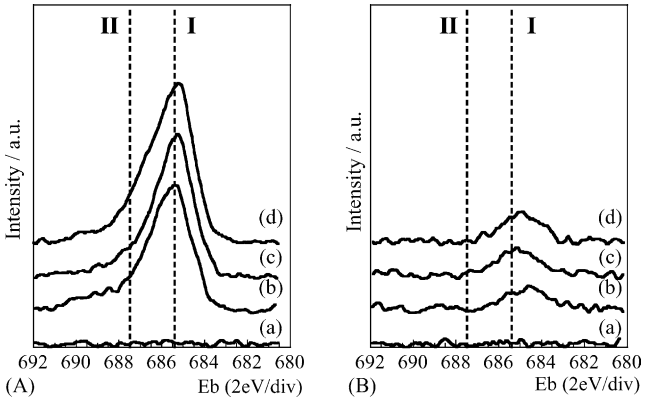

Fig. 5. XPS spectra of F1s electron in $LiMn_2O_4$ untreated (a) and treated with 1.3 kPa-F_2 at room temperature, RT (b), 6.6 kPa-F_2 at RT (c), 13.2 kPa-F_2 at RT (d) ((A) before and (B) after Ar^+ etching).

Fig. 7 shows the discharge curves in the first cycle of $LiMn_2O_4$ fluorinated under various conditions. The shape of the discharge curves are similar to each other. But the discharge capacity changed by the fluorination. The results of the charge/discharge tests are summarized in Table 1. F/O ratio measured by XPS is also shown in the table. The efficiency, i.e., the ratio of charge to discharge capacities is

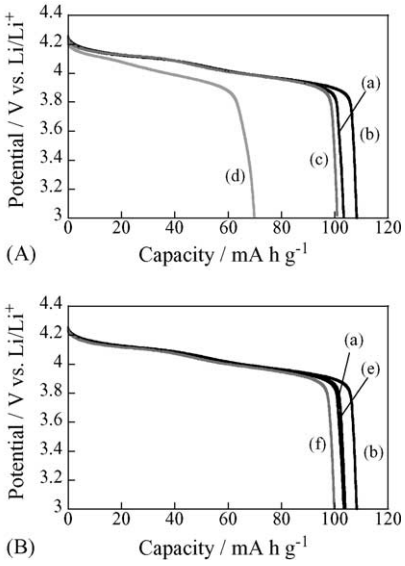

Fig. 7. Discharge curves of $LiMn_2O_4$ untreated (a) and treated with 1.3 kPa-F_2 at room temperature, RT (b), 1.3 kPa-F_2 at 373 K (c), 1.3 kPa-F_2 at 473 K (d), 6.6 kPa-F_2 at RT (e), 13.2 kPa-F_2 at RT (f) ((A) reaction temperature dependence, (B) F_2 pressure dependence). Charge and discharge was carried out at a constant current corresponding to the rate of 0.3 °C. Cut off potential was set at 4.5 V.

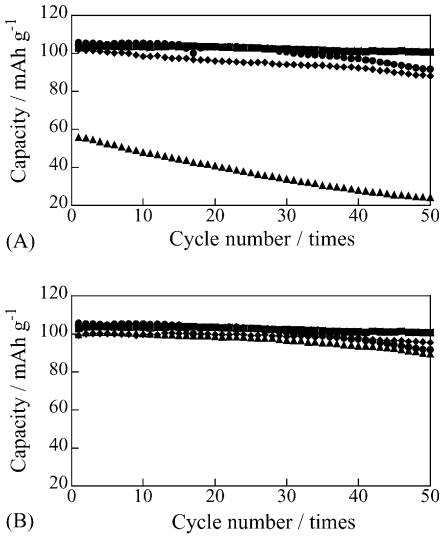

Fig. 8. Change in discharge capacities along cycle number of $LiMn_2O_4$ untreated (●) and with 1.3 kPa-F_2 at room temperature, RT (■), 1.3 kPa-F_2 at 373 K (◆) and 1.3 kPa-F_2 at 473 K (▲) in (A), and untreated (●) and with 1.3 kPa-F_2 at room temperature, RT (■), 6.6 kPa-F_2 at RT (◆) and 13.2 kPa-F_2 at RT (f) (▲) in (B). Charge and discharge was carried out at a constant current corresponding to the rate of 0.3 °C. Cut off potential was set at 4.5 V.

improved by fluorinating the surface. Especially, $LiMn_2O_4$ fluorinated with 6.6 kPa-F_2 at RT had the efficiency higher than 95%. Fluorination of the $LiMn_2O_4$ surface with F_2 caused the increase of the discharge capacity. Average potentials during the discharge of $LiMn_2O_4$ fluorinated with 1.3, 6.6 and 13.2 kPa-F_2 at RT were more noble, and those with 1.3 kPa-F_2 at 372 and 473 K were less noble than that of untreated one. This seems that an excess fluorination causes the formation of a resistive film which consist of some fluorides on the surface. The discharge capacity of $LiMn_2O_4$ fluorinated with 1.3 kPa-F_2 at RT was 6% larger than that of untreated one. The improvement of the discharge capacity by the fluorination with F_2 was larger than that with NF_3 in our previous study [10]. The change in the discharge capacities during 50 cycles are shown in Fig. 8. The loss of discharge capacity during 50 cycles were 13, 2, 14, 57, 4 and 10% for $LiMn_2O_4$ untreated and fluorinated with 1.3 kPa-F_2 at RT, 1.3 kPa-F_2 at 373, 1.3 kPa-F_2 at 473 K, 6.6 kPa-F_2 at RT and 13.2 kPa-F_2 at RT, i.e., (a)–(f) in Fig. 6. This loss was in the order of (b) < (e) < (a) < (c) < (f) < (d). As shown in Table 1, F/O ratios were in the order of (b) < (c), (e) < (f) < (d). Consequently, the results of XPS measurements and the charge/discharge tests were closely related with each other. In addition, the discharge capacity of 109.3 mA h g^{-1} and the loss of 2% in the discharge capacity during 50 charge/discharge cycles were totally better than those obtained for $LiMn_2O_4$ fluorinated with NF_3 reported in our previous paper [10].

3. Experimental

Fluorine gas (purity: 99.4–99.7%) used in the present study was supplied by Daikin Co., Ltd. $LiMn_2O_4$ having the average diameter of 5 μm was used. The surface of $LiMn_2O_4$ was treated with F_2 at room temperature, 373 and 473 K for 1 h. The reaction temperature was set. XPS spectra were obtained by using ESCA750 (Shimadzu).

Table 1
Charge/discharge properties in first cycle and the ration of F/O on the sample surface measured by XPS

Sample	Capacity (mA h g^{-1})		Efficiency (%)	V_{ave}[a]/V vs. Li/Li^+	F/O from XPS
	Charge	Discharge			
Untreated	111.4	103.4	92.9	3.98	0.0
1.3 kPa-F_2, RT	117.3	109.3	93.2	3.99	1.4
1.3 kPa-F_2, 372 K	109.5	101.1	92.2	4.01	1.7
1.3 kPa-F_2, 473 K	85.1	69.9	82.1	3.00	2.4
6.6 kPa-F_2, RT	110.4	105.0	95.1	3.98	1.8
13.2 kPa-F_2, RT	105.5	99.9	94.7	3.08	2.1

[a] Average discharge potential during discharge.

Argon ion sputtering was carried out at 2 kV with 25 mA for 30 min. Three-electrode cell (Hokuto Denko Co., F type cell) was used for the electrochemical measurements. The sheet of the mixture consisting of $LiMn_2O_4$, acetylene black and polyterafluoroethylene in weight ratios of 5:4:1 was expanded onto Ti mesh on the can made by SUS304. The electrolyte was 1.0 mol dm^{-3} $LiClO_4$/PC + DME (1:1 in volume). The Li foil was used as reference and counter electrodes. After setting up the test cell in an Ar bag, the electrochemical measurements were carried out at 25 °C in an air by using HJ101SM6 and HZ3000 (Hokuto Denko Co.).

References

[1] T. Ohzuku, in: G. Pistoia, Lithium Batteries: New Materials, Developments, Perspectives, Amsterdam, 1994, pp. 239–280.
[2] W. Ebner, D. Fouchard, L. Xie, Solid State Inonics 69 (1994) 238–256.
[3] D. Guyomard, J.M. Tarascon, Solid State Inonics 69 (1994) 222–237.
[4] M.M. Thackeray, A. de Kock, M.H. Rossouw, D. Liles, R. Bittihn, D. Hoge, J. Electrochem. Soc. 139 (1992) 363–366.
[5] Y. Todorov, C. Wang, B.I. Banov, M. Yoshio, Electrochem. Soc., Proc. Paris 97–18 (1997) 176–184.
[6] N. Hayashi, H. Ikuta, M. Wakihara, J. Electrochem. Soc. 146 (1999) 1351–1354.
[7] T. Ohzuku, A. Ueda, J. Electrochem. Soc. 141 (1994) 2972–2977.
[8] S. Yonezawa, M. Takashima, M. Ohe, T. Iida, Abst. of 2000 International Chemical Congress of Pacific Basin Societies, INOR-1484, 2000.
[9] M. Takashima, S. Yonezawa, M. Ozawa, Mol. Cryst. Liq. Cryst. 388 (2002) 153–159.
[10] S. Yonezawa, M. Ozawa, M. Takashima, Tanso 205 (2002) 260–262.
[11] D.B. Jiang, Y. Kogo, I. Tari, Electrochemistry 67 (1999) 359–363.
[12] T. Nakajima, in: T. Nakajima (Ed.), Fluorine–Carbon and Fluoride–Carbon Materials: Chemistry, Physics, and Applications, Marcel Dekker, New York, USA, 1995, Chapter 1.
[13] T. Nakajima, M. Koh, R.N. Singh, M. Shimada, Electrochim. Acta 44 (1999) 2879–2888.
[14] K.L. Choy, J. Zhao, Scr. Mater. 39 (1998) 839–845.
[15] M. Takashima, S. Yonezawa, S. Hirano, M. Iino, T. Unishi, A. Sumiyama, J. Fluorine Chem. 72 (1995) 55–59.
[16] M. Takashima, S. Fukami, Y. Nosaka, T. Unishi, J. Fluorine Chem. 57 (1992) 131–138.
[17] M. Takashima, M. Amaya, G. Kano, S. Fukami, J. Fluorine Chem. 46 (1990) 7–19.